FliPASED
WWW.FLIPASED.EU

D4.3 Report on Quantified Design Benefits, as compared with Reference

Thiemo Kier, Yasser Meddaikar, Matthias Wuestenhagen (DLR), Milán Bárczi, Balint Vanek, Béla Takarics (SZTAKI), Charles Poussot-Vassal (ONERA), Fanglin Yu (TUM)

GA number:	815058
Project acronym:	FLIPASED
Project title:	FLIGHT PHASE ADAPTIVE AEROSERVO-ELASTIC AIRCRAFT DESIGN METHODS
Funding Scheme: H2020	**ID:** MG-3-1-2018
Latest version of Annex I:	1.2 released on 13/12/2022
Start date of project: 01/09/2019	**Duration:** 46 Months

Lead Beneficiary for this deliverable:	DLR
Last modified: 13/09/2023	**Status:** Submitted
Due date: 30/06/2023	

Project co-ordinator name and organisation:	Bálint Vanek, SZTAKI
Tel. and email: +36 1 279 6113	vanek@sztaki.hu
Project website:	www.flipased.eu

Dissemination Level		
PU	Public	X
CO	Confidential, only for members of the consortium (including the Commission Services)	

“This document is part of a project that has received funding from the European Union’s Horizon 2020 research and innovation programme under grant agreement No 815058.”

Glossary

ADEBO	Aircraft Design Box
ASE	Aeroservoelastic
AFS	Active Flutter Suppression
CAD	Computer-aided Design
CFD	Computational Fluid Dynamics
CFRP	carbon-fiber-reinforced polymers
CPACS	Common Parametric Aircraft Configuration Schema
EAS	Equivalent Airspeed
FCC	Flight Control Computer
GFEM	Global Finite Element Model
GLA	Gust Load Alleviation
HIL	Hardware-in-the-Loop
HTP	Horizontal Tail Plane
LTI	Linear Time-invariant
MDO	Multidisciplinary Design Optimization
MLA	Manoeuvre Load Alleviation
PDF	Portable Document Format
PID	Proportional-Integral-Derivative
RCE	Remote Component Environment
SAS	Stability Augmentation System
SFC	Specific Fuel Consumption
SMR	Short and Medium Range
SUAVE	Stanford University Aerospace Vehicle Environment
UAV	Unmanned Aerial Vehicle
UNICADO	University Conceptual Aircraft Design and Optimization
VTP	Vertical Tail Plane

Table of contents

List of Figures

1 Objective of ScaleUp Task

The overall objective function for the scale-up task will be based on evaluation of the mission criteria range in the cruise segment, as mentioned in the previous section. This way two primary design goals can be addressed. The first goal is to minimize the aerodynamic drag. Specifically, the induced drag is addressed by high aspect ratio wing designs. However, the resulting slender wing structures tend to be very flexible and defueling the wing tanks change the mass distribution and in turn the shape of the wing. To counteract the detrimental effect on the induced aerodynamic drag, active wing shape control deflects the control surfaces to restore a drag optimal lift distribution for the changing wing mass. The second goal is to minimize the structural weight. This can be achieved by employing active load alleviation control laws to minimize design loads for manoeuvres as well as gusts and turbulence in combination with passive methods for load alleviation such as aeroelastic tailoring. Furthermore, the aforementioned high aspect ratio wings are more prone to an adverse fluid structure interaction called flutter. Conventionally, this is addressed by increasing the wing stiffness or placing additional mass in suitable locations. The employment of Active flutter suppression makes a design feasible in case flutter occurs within the extended certification flight envelope.

The technologies employed are:

- Manoeuvre Load Alleviation Control Functions
- Gust Load Alleviation Control Functions
- Active Flutter Suppression
- Wing Shape Control for drag reduction in cruise
- Passive Load Alleviation with aeroelastic tailoring
- Control surface layout (eight trailing edge surfaces)

To assess the benefits of the mentioned active control technologies, the mission is analyzed at multiple points of the flight envelope and via various mission profiles, i.e. different mass cases due to defueling, as mentioned in the previous paragraph. This Assessment will be done by a simple metric using the Breguet equation for the cruise segment of the aircraft mission, allowing for comparative studies between the different design of the collaborative workflow. The performance evaluation is not meant for an absolut performance evaluation in comparison with other aircraft types.

The conjecture is that inclusion of active control theory in the design phase leads to very different wing designs and a large overall fuel savings.

2 Reference Aircraft Model

The scale-up task is performed with an already feasible, optimized aircraft baseline. It was decided earlier to select the already available D150 aircraft model. A brief description of the aircraft is recapped below.

D150: DLR 150Pax Model (A320 like)

The D150 configuration was developed within the DLR project VAMP [11]. It is comparable to the Airbus A320-200 aircraft. Data published by the manufacturer and input data to the preliminary design

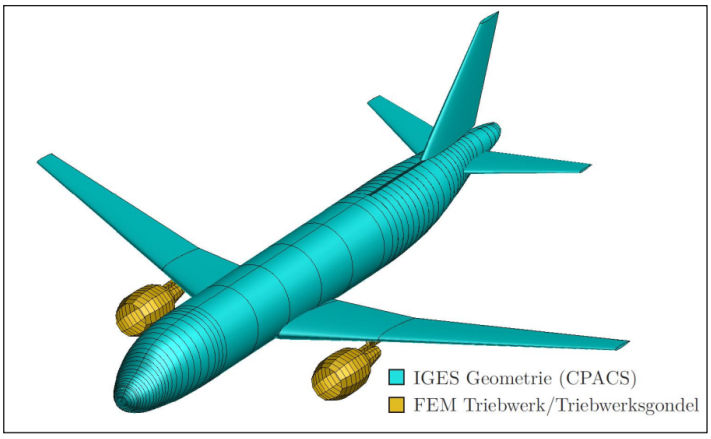

Figure 1: IGES-geometry of the D150-configuration

program PrADO for the application example Airbus A320, are collected for the D150 configuration [8]. Its geometry is shown in Figure 1. Table 1 lists some parameters of the D150 configuration. The cruise speed V_C and cruise Mach number M_C are assumed to be equal to the maximum operational speeds V_{MO} and M_{MO}. The values for V_{MO} and M_{MO} for the Airbus A320 are given in the EASA Type-Certificate Data Sheet [4]. The dive speed V_D is determined using the diagram of worksheet LTH BM 32 100-05 of the Luftfahrttechnischen Handbuch (LTH), and the dive Mach number $M_D = M_C + 0.07$ from the Acceptable Means of Compliance AMC 25.335(b)(2) of CS25.

The three airfoil profiles are used for the four profile sections. They originate from the geometry of the DLR-F6 configuration. The DLR-F6 configuration is similar to the geometry of the Airbus A320. It was developed in the 1980s as a publicly-available geometry for aerodynamic studies.

Using the D150 configuration provides the following advantages and disadvantages.
For:

- DLR-proprietary configuration
- Relevance to industry - short/medium-range (SMR) configuration
- CPACS dataset available and maintained across various project developments
- Experience from several other projects involving D150 model
- No restrictions pertaining to publication

Against:

- Aero-loft not suitable for CFD simulations - aerodynamics restricted to potential flow methods

The DLR-D150 was selected by the consortium as the preferred reference model for the scale-up task. All considered reference models are found in deliverable D1.5.

The primary reason for choosing the D150 is its relevance to industry and on-going research activities in different projects. An A320-like configuration is considered to be a SMR aircraft. Moreover, the availability of a CPACS dataset and freedom pertaining to publications are advantageous.

Wing	
Surface area	$122.3 m^2$
Span	$33.91 m$
Reference chord	$4.19 m$
Aspect ratio	9.4
Taper ratio	0.246
Sweep angle at 25% chord line	24.94^o
HTP	
Area	$30.98 m^2$
Span	$12.45 m$
Aspect ratio	5.0
Taper ratio	0.33
Sweep angle at 25% chord line	28.0^o
VTP	
Area	$21.51 m^2$
Span	$5.87 m$
Aspect ratio	1.6
Taper ratio	0.35
Sweep angle at 25% chord line	35.0^o
Operational empty weight (OEM)	$40638 kg$
Maximum zero-fuel weight (MZFM)	$60500 kg$
Maximum take-off weight (MTOM)	$72500 kg$
Cruise Mach number	0.78
Cruise speed / Mach number	$180 m/s$ EAS, Mach 0.82
Dive speed / Mach number	$209 m/s$ EAS, Mach 0.89
Maximum flight level	$12500 m$

Table 1: Main parameters of the D150-configuration

The drawback of not having a good enough aero loft to carry out CFD simulations as in the case of the D150, is mitigated by the fact that only potential flow methods are intended to be employed. The target performance optimization goal in FLiPASED is the reduction of induced drag, i.e. drag due to lift distribution. However, the developed tools and methods are intended to be applicable even in a potential future workflow involving high fidelity CFD simulations.

The decision to choose the DLR-D150 is in line with multiple local on-going activities and projects to iterate on future SMR (Short Medium Range) aircraft configurations . Among others, one can count:

- VirEnfREI-DLR - LuFo funded project involving DLR and Airbus. It involves establishing an MDO framework for aircraft design with respect to industrial requirements and its application to the design of a high aspect ratio SMR aircraft.
- MuStHaF-DLR - LuFo funded project involving DLR institutes. It is targeted towards future high aspect ratio SMR aircraft configurations considering different wing technologies, e.g. multi-functional control surfaces, control algorithms for AFS and online flutter stability monitoring.
- MAJESTIC - DGAC funded project involving ONERA and Airbus. The project is concerned with the aeroelastic modelling methodology and control design for flutter phenomena. The considered use-case is a generic single aisle high aspect ratio configuration.

Apart from this, Dassault-Aviation from the Scientific Advisory Group in FLIPASED had expressed interest during the initial phase of the project in a potential narrow-body aircraft for scale-up studies as opposed to wide-body aircraft.

3 Process

The Scale-up task includes many different tools which have to be connected. The interactive workflow is depicted in Figure 2. At first the aspect ratio is the considered input parameter. The different blocks are described below.

3.1 CPACS dataset and conceptual analysis

The CPACS dataset for D150 has already been obtained and serves as a foundation for the project. However, to achieve the project's objectives, the initial three control surfaces have been expanded to a total of ten. Additionally, to explore the impact of aspect ratio on aircraft performance, various CPACS datasets have been generated.

Before progressing to the aeroelastic modeling phase, the CPACS dataset undergoes a thorough examination in the conceptual design block. This evaluation aims to ensure the configuration's stability in terms of flight dynamics. For this purpose, the open-source tool SUAVE [2] is utilized to conduct a feasibility check. Further information on this process will be presented in Section 5.

4 Parameteric Study

Instead of doing an elaborate Optimization Task in an MDO context a parameter sweep of the most essential parameters is used to determine the benefits of active control technologies.

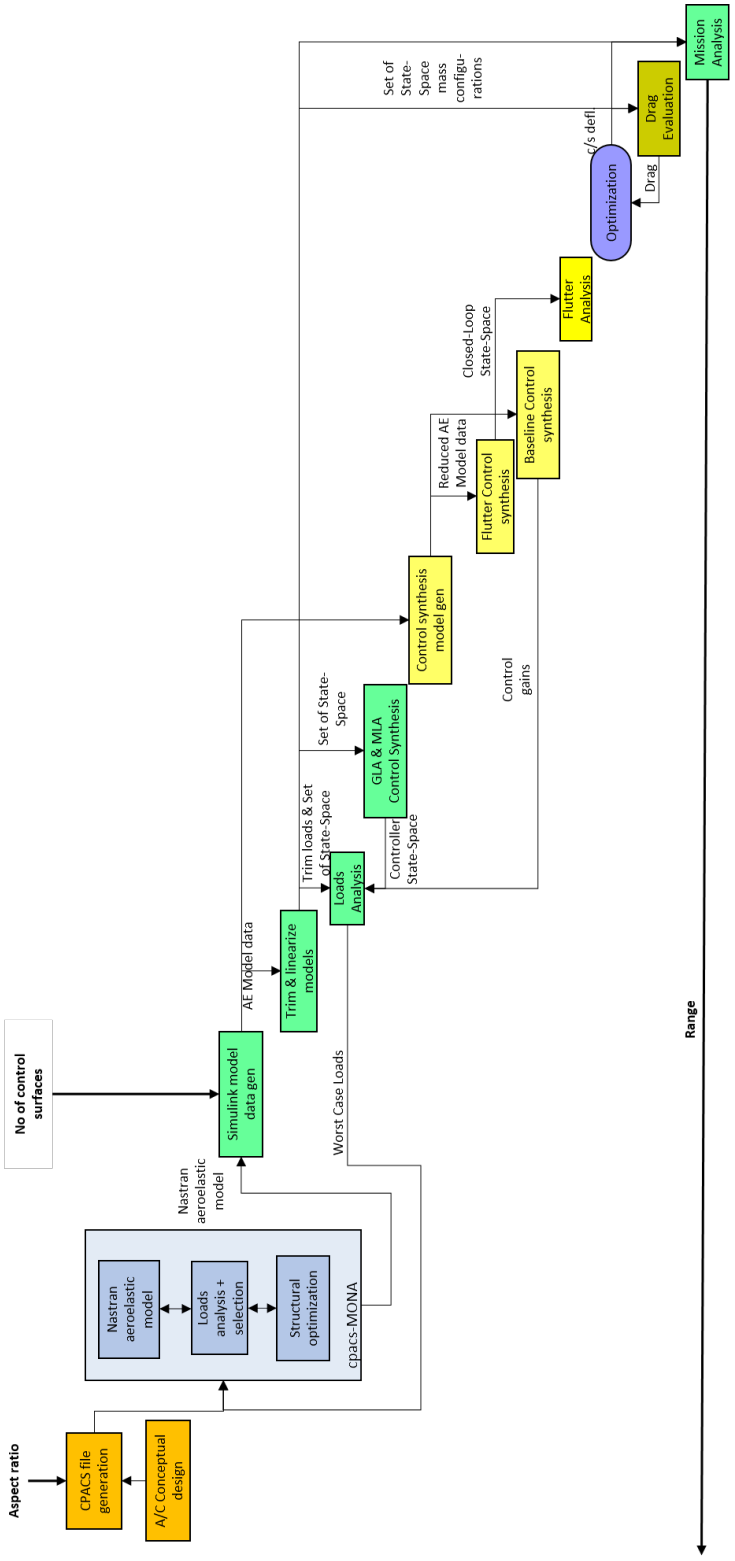

Figure 2: Diagram of the scale-up Workflow

The parameter sweep is done for the aspect ratio of the wings, since this is the primary focus of many aircraft manufactures. The increased aspect ratio has a substantial effect on the flexiblity of the wings which might be prone to flutter instabilities, reduced roll controlablity and increased loads due to gusts and turbulence.

5 Conceptual Design

As previously mentioned, the main objective is to examine trends in relation to varying aspect ratios. Due to time constraints, the range of aspect ratios has been limited to 9.4 (Fig. 3) and 18.4 (Fig. 4). The initial CPACS dataset has an aspect ratio of 9.4. The value of 18.4 is chosen as a reasonably high value that may be achievable with improved technology in the future. In total, six different configurations will be investigated to demonstrate a meaningful trend in relation to aspect ratio.

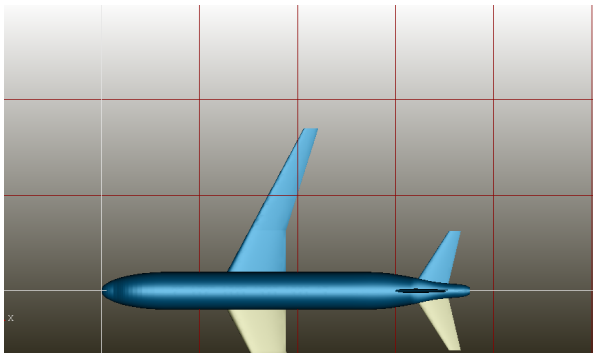

Figure 3: D150 AR 9.4

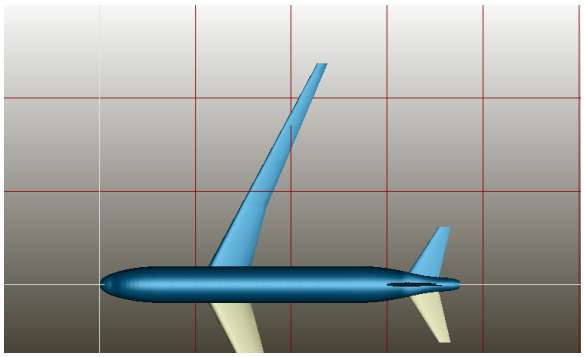

Figure 4: D150 AR 18.4

To prevent the design space from becoming excessively large and to control the influencing factors, certain preconditions have been defined. One of these preconditions is to maintain a similar wing planform by keeping the sweep angle and taper ratio constant. Additionally, the wing area is kept constant to ensure consistent wing loading, thereby avoiding any significant impact on aerodynamic performance and load analysis of the wing. By imposing these preconditions, the focus can be directed toward investigating the influence of varying aspect ratios while minimizing other potential variables.

In order to vary the aspect ratio, adjustments are made to the wing's span. The first segment of the wing, which lies within the fuselage, maintains a constant length since the fuselage itself remains unchanged. Therefore, only the segment of the wing outside of the fuselage is scaled according to the desired aspect ratio. To ensure the wing area remains constant, the root chord is adjusted as the wing span is modified. This approach allows for controlled changes in aspect ratio while maintaining a consistent wing area and fuselage dimensions.

As the aspect ratio increases, the wing span is extended accordingly and the wing becomes more slender. This change, along with the sweep angle, causes the aerodynamic center to shift further toward the rear. Consequently, it can affect the flight dynamics of the aircraft. To ensure that the aircraft remains stable and to facilitate the design of a baseline controller, a stability check is conducted using SUAVE [2], an aircraft design tool developed by Stanford University.

During this stability check, the wing position is adjusted longitudinally to maintain a constant neutral point. By keeping the neutral point consistent, the stability characteristics of the aircraft can be preserved despite the changes in aspect ratio and wing configuration. This process helps ensure that the aircraft remains controllable and stable throughout its flight envelope. If this is not sufficient, tail volume

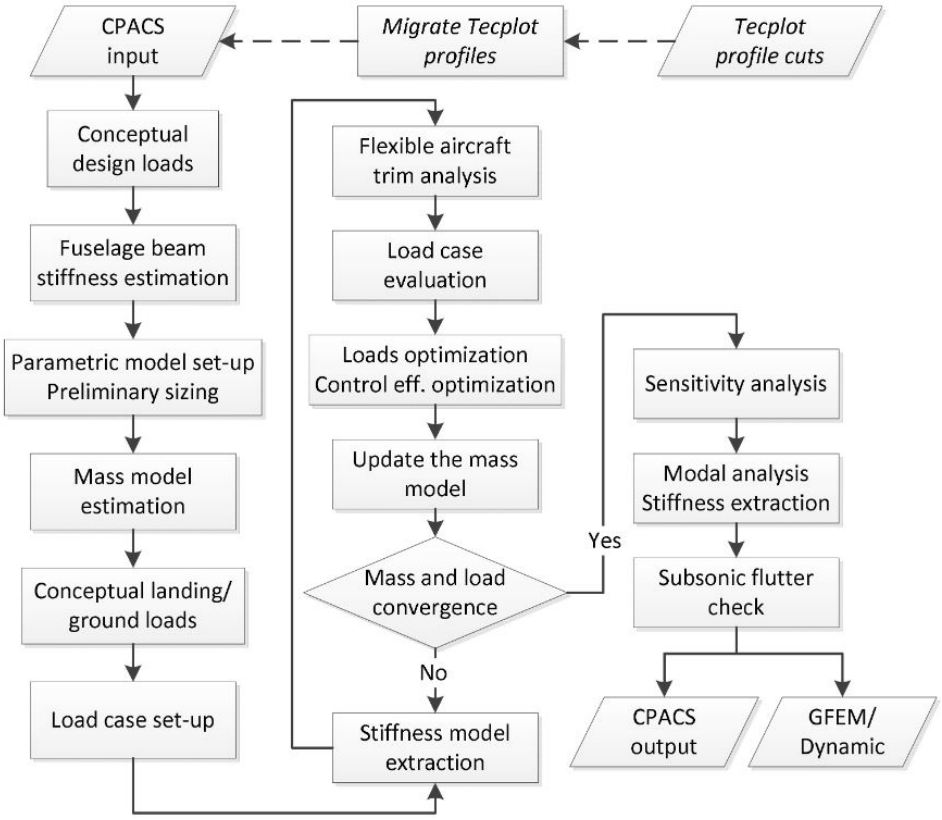

Figure 5: Process flow of cpacs-MONA

can be sized to fulfill the stability requirements.

6 Model generation and structural sizing

The parameterized aeroelastic structural design process cpacs-MONA [9, 10] is used for the scale-up task within FLIPASED. The tool is used to perform a simultaneous structural and aeroelastic design of the load carrying structure of an aircraft configuration. The process includes preliminary mass and loads estimation based on conceptual design methods followed by a parameterized set-up of simulation models and an optimization model. These models are used for a comprehensive loads analysis followed by a component wise structural optimization. The latter takes stress, strain, buckling and control surface efficiency as constraints into account. The detailed structural modelling allows also for the use of well-established structural optimization methods. The data basis for the simulation models and the various analyses is a suitable CPACS dataset. A schematic of the different tools incorporated within cpacs-MONA are shown in Figure 5.

Within WP4, the following are the primary steps planned with cpacs-MONA.

1. For each variant of the DLR-D150 and its associated CPACS dataset, the first aircraft loads and sizing step will be performed. The loads are without inclusion of MLA/GLA. The ensuing aircraft data files as described in Section 6 are passed on the partners downstream of the MDO toolchain.

2. For a set of input loads (closed loop loads with MLA/GLA) from the second iteration onwards, an aggregate set of loads is setup together with ground loads, followed by a loads selection process. The structural sizing is performed without executing any of the upstream tools shown in Figure 5. The ensuing aircraft data files are once again transferred.
3. For the final design in each of the runs, an open loop flutter analysis using the PK-solver in NASTRAN is performed.

In the first internal structural optimization step, the structure is optimized using a set of open-loop loads.

Maneuver loads, gust loads and ground loads are considered. A flight envelope is set up according to CS25.335 requirements for the given or approximated design speeds V_C/M_C and V_D/M_D, where V_C is set to V_{MO}. V_{MO} is either considered from the CPACS dataset or approximated based on the given target cruise speed M_{cruise} at the service ceiling level. The stall speed V_S and the maneuver speed V_A are estimated based on c_{lmax} , c_{lmin} and $c_{l\alpha}$. Load cases for maneuver and gust are finally defined as a combination of distinct flight points (speed and altitude), a load factor or a gust definition, and a mass configuration. For the maneuver loads, symmetric pull-up and push-down as well as yawing and rolling are considered.

7 Loads Analysis and Dynamic Simulation Model setup

The tool used for dynamic model generation and dynamic closed loop loads analysis is the DLR tool VarLoads. In a first step, the open loads loads are recalculated to ensure consistency with the previous sizing step. The loads are compared with the loads from the previous calculations with cpacs-MONA to confirm the stiffness and mass model.

The performance assessment of the GLA and MLA control relies on the loads, denoted as P_c, experienced by the aircraft structure during gust encounters. These loads are determined using the force summation method (FSM), expressed as

$$P_c = T_{cg}\left(P_g^{\text{ext}} - P_g^{\text{iner}}\right). \tag{1}$$

Here, P_g^{ext} and P_g^{iner} represent the external and inertial loads, respectively. The incremental loads from all load monitoring points are aggregated and transformed to the loads coordinate system using the transformation matrix T_{cg} [1, 7].

The gust input to the aerodynamic model consists of vertical 1-cosine gust profiles, characterized by the gust zone velocity $U_{z,t}(t)$ and acceleration $\dot{U}_{z,t}(t)$, defined as

$$\begin{aligned} U_{z,t}(t) &= \begin{cases} \frac{\bar{U}_t}{2}\left(1-\cos\left(\frac{\pi}{H_t}\left(U_\infty t - x_z\right)\right)\right), & \text{if } \frac{x_z}{U_\infty} \le t \le \frac{2H_t + x_z}{U_\infty} \\ 0, & \text{otherwise} \end{cases} \\ \dot{U}_{z,t}(t) &= \begin{cases} \frac{\bar{U}_t \pi}{2H_t} U_\infty \sin\left(\frac{\pi}{H_t}\left(U_\infty t - x_z\right)\right), & \text{if } \frac{x_z}{U_\infty} \le t \le \frac{2H_t + x_z}{U_\infty} \\ 0, & \text{otherwise.} \end{cases} \end{aligned} \tag{2}$$

Here, $\bar{U}t$ represents the maximum gust intensity, Ht is the gust half length, and x_z denotes the position along the aircraft [3]. The gust profile is traversed by the aircraft, as illustrated in Figure 6. Simulation of the 1-cosine gust encounters for the determined critical load cases provides the critical loads. Comparison of the calculations with the ones received from cpacs-MONA allows to validate the workflow up

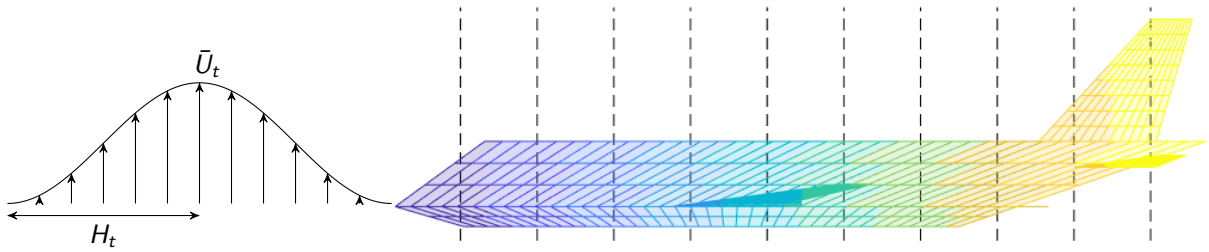

Figure 6: 1-cosine gust and aircraft gust zones.

to this point.

For the manoeuvre loads the aircraft is trimmed for the most critical manoeuvres. The trim solution then provides the corresponding critical loads.

For the subsequent control synthesis tasks the open-loop nonlinear simulation model is trimmed and linearized to obtain states space models. Model order reduction is applied to these models to make them suitable for control law synthesis.

The flight points of the state-space models for the design of these load alleviation functions (LAF) are chosen according to the list of the computed load cases. The flight points for the active flutter suppression control laws are based on the 15% extended fight envelope required for certification of the aircraft according to CS 25 [3].

8 Control Law design for Load Alleviation Functions

8.1 Gust Load Alleviation

The GLA control laws are designed for reduction of the wing root bending due to 1-cosine gusts. The control law is assumed to be a single gain matrix, which relates the onboard measurements to control surface deflections. In Figure 7 the control surfaces employed for GLA are framed in magenta. Each wing possesses ten aileron-like control surfaces. For simplification the control surfaces are grouped by two, which provides five control surfaces per wing. Furthermore, the elevator control surfaces are used for GLA as well. As vertical gust cases are considered exclusively, allocation of symmetrically corresponding control surfaces of the aircraft is possible. The output provided to the GLA controller is solely the z-acceleration from the fuselage IMU. Its orientation is depicted by the coordinate axes in Figure 7.

The GLA control law is determined by an optimisation. Based on a couple of gust encounters, covering gust half lengths of $30\,\mathrm{ft}$ to $350\,\mathrm{ft}$, the maximum occurring wing root bending moment (WRBM) $P_{c,\mathrm{mx}}$ is determined. Thus, the main objective of the optimisation is to minimise the WRBM over all simulated gust encounters. Additionally, the control law should not cause to strong vibrations. Therefore, the maximum integral of the WRBM for all gust encounters should not exceed $90\,\%$ of the maximum integral of the WRBM in open-loop. Adding this constraint to the optimisation problem also prevents an unstable closed-loop behaviour.

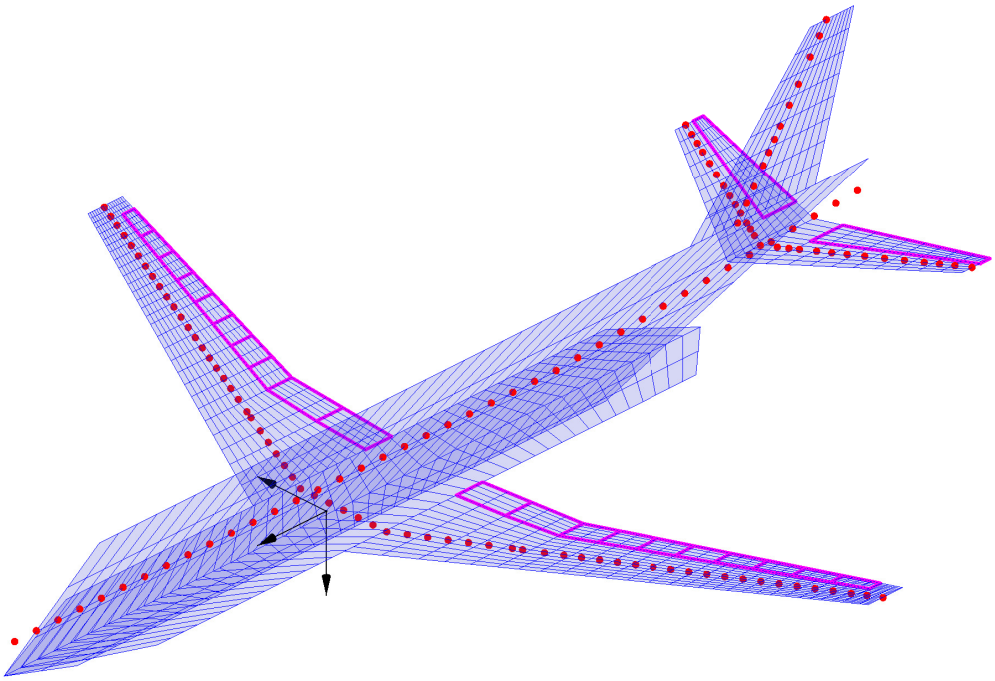

Figure 7: D150 flexible aircraft model defined by the structural grid (red), the aerodynamic panel model (blue), the deployed control surfaces for GLA (magenta), and the IMU coordinate system location and orientation (black).

8.2 Manoeuvre Load Alleviation

For certification of an aircraft, it has to be demonstrated that its structure can withstand the loads acting on it without damage. In order to design the structure accordingly, a so called loads envelope has to be computed. One of the critical load conditions comprising the loads envelope is the symmetrical pull up manoeuvre. For large transport aircraft, this condition is specified in the paragraphs CS 25.331 and CS 25.333 of the CS-25 issued by the EASA. One way of reducing the resulting wing root bending moment and hence the structural weight of the wing, is to shift the center of the lift distribution inboard by deflecting the control surfaces. This function is known as Manoeuvre Load Alleviation (MLA).

The objective is to find the optimal control surface scheduling to minimize the wing bending moment over the wing span. In particular the reduction of the integrated bending moment at the wing root will result in the most structural weight savings and is hence the indicator which control surface allocation to choose.

The aircraft model is trimmed for a pull-up manoeuvre with the resulting pitch rate to reach the desired load factor. The maximum deflections for the 10 wing trailing edge surfaces were set to be 10 deg upward. Such a setup requires a constraint optimization with the objective function minimizing the resulting wing root bending moment by symmetric deflection of the trailing edge control surfaces. Ultimately, to reduce the root bending moment the center of lift has to be shifted inboard. Physically, that means that the outboard lift is decreased, by upward deflection of the outer control surfaces.

Since the manoeuvre loads are computed by trimming the aircraft for specific flight condition like pull-up, push-over and roll manoeuvres, the design of a dynamic control manoeuvre load alleviation law is not necessary for the subsequent loads analysis. For the manoeuvre loads the allocation of the control

surfaces however plays an essential role. To find the optimal spanwise cross-over location, where neutral position changes to full upward deflection of the trailing edge control surfaces, 11 discrete configurations were examined. The reference case 00 is without any MLA function, i.e. no deflection of the control surfaces. For configuration 01 all trailing edge surfaces are deflected upwards -10 deg. The configs 02 through 11 consecutively return more control surfaces from inboard to outboard to their neutral position, until for configuration 10 only the outermost aileron is deflected upwards.

The configuration 03, where all but the two innermost flaps are deflected upward is the configuration with the minimum wing root bending moment, as show in figure 8. The two flaps that are not deflected are inboard of the trapezoidal kink of the wing. The control surface layout is depicted in figure 7.

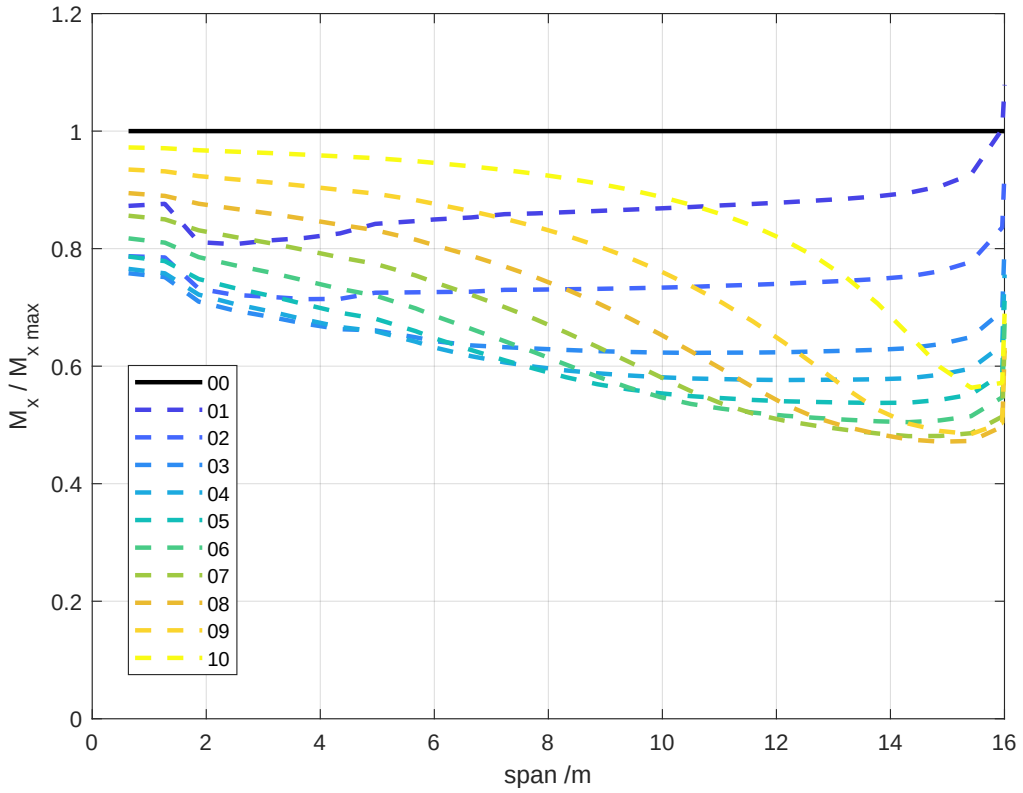

Figure 8: wing bending moment distribution of the various MLA control surface configurations normalized by the unreduced bending moment distribution.

Please note that the sole selection criterion for the MLA control surface allocation is based on the resulting wing root bending moment. In the described workflow no other constraints have been considered. Such constraints could be for instance the trade off between wing loads and horizontal tail loads, buffeting constraints regarding the maximum lift coefficient at the dive Mach number, aerodynamic efficiency considerations of the control surfaces in a transonic flow regime, detrimental effects on a benign stall behavior, etc.

9 Closed loop Loads Analysis

Using the control laws of the previous step, the loads analysis is executed for the closed loop aircraft with the LAF active once again. Here, it is assumed that the determined critical load cases in open-loop are still the most critical ones for closed loop.

In order to determine the most critical load cases the flight envelope of the D150 aircraft is gridded for different speeds and altitudes. This is performed for various mass cases. The critical gust loads are determined dynamically. Several gradient lengths ranging from $30\,\mathrm{ft}$ to $350\,\mathrm{ft}$ of 1-cosine gust encounters are simulated as specified in CS25.341 and the maximum gust loads experienced at different monitoring points are determined. The most critical loads are found for different gust half lengths at cruise speed and $8000\,\mathrm{m}$ altitude for the maximum take-off mass configuration.

The previously described synthesis of GLA control focusses solely on the obtained critical load cases. Solving the optimisation problem then provides the control gains. Figure 9 shows the difference between the open-loop and closed-loop gust response of the WRBM for the critical load cases. It is visible, that

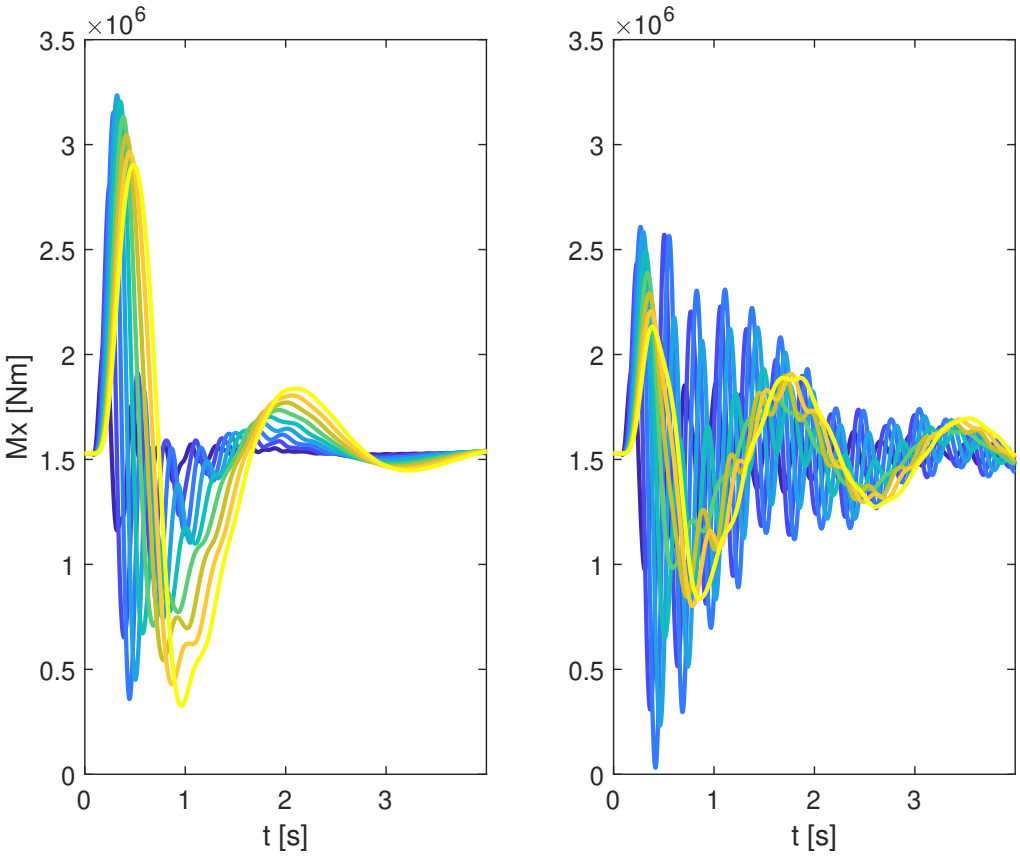

Figure 9: Comparison of the WRBM without (left) and with (right) GLA.

the maximum WRBM can be strongly reduced by around $80\,\%$. The decrease in vibration in closed-loop

is not as strong as in open-loop, however, it is found to be in an acceptable range.

The same is done statically for the manoeuvre loads. The maximum manoeuvre loads are found by trimming the aircraft for the predefined critical manoeuvres.

In both cases, the loads of the open and closed-loop system are compared with GLA and MLA. The higher the difference the higher the potential for improvements in structural sizing. Figure 10 depicts the bending moment along the wing span, which is normalised with the maximum open-loop bending moment which is observed at each wing span position due to gust encounter. Thus, if $M_x/M_{x,\max}$ is 1

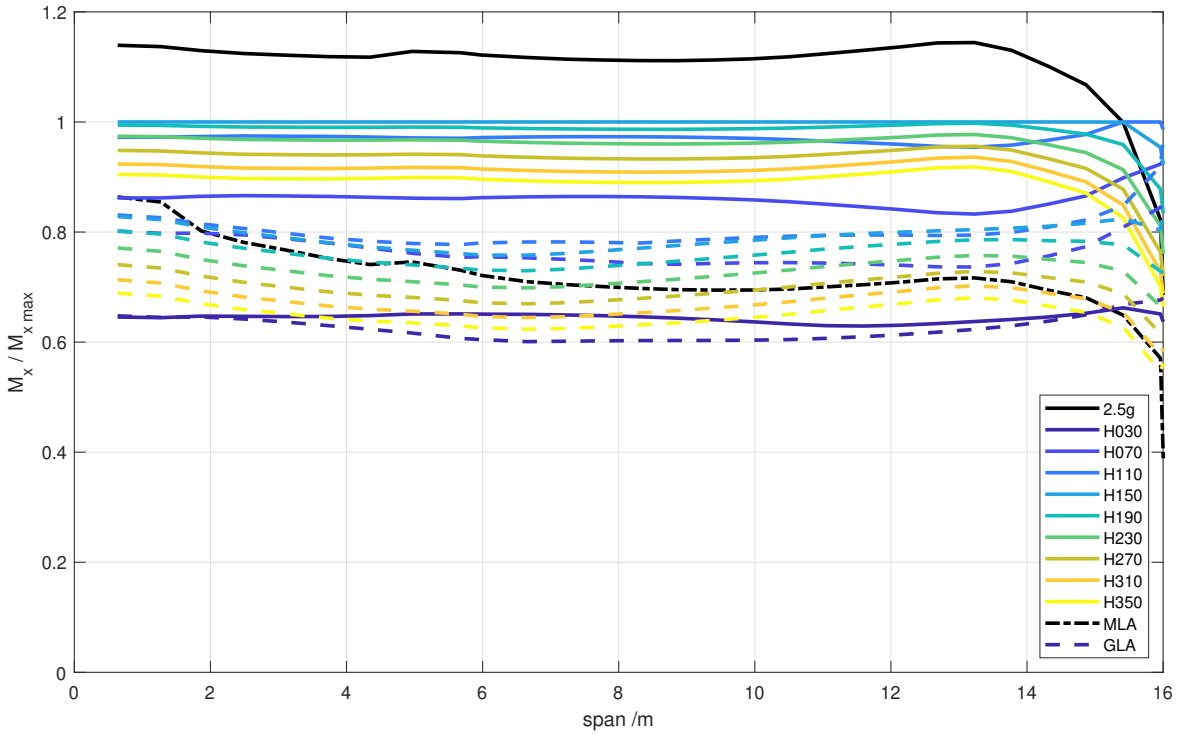

Figure 10: Critical load cases without (solid) and with (dashed) MLA and GLA.

the loads are most critical at the considered position with respect to gusts. It is visible that from the wing root up to the wing tip, gusts featuring a half length of $150\,\mathrm{ft}$ are the most relevant. Application of GLA shifts the bending moment by approximately $20\,\%$. Close to the wing tip the load reduction is not as high. However, from a structural sizing and mass reduction point of view the outer wing is not that relevant.

The manoeuvre most critical for the bending moment is assumed to be a $2.5\,\mathrm{g}$ pull-up at dive speed. As can be seen, it even exceeds the critical gust loads by approximately $15\,\%$. With the proposed MLA it is possible to shift the manoeuvre loads to a similar range like the alleviated gust loads. Right at the wing root it remains the driving load case, but becomes uncritical towards the wing tip.

10 Structural Sizing

In this step, the resulting weight savings due to the active control technologies are determined. Three levels of fidelity are defined for this step with progressing maturity and complexity.

1. Rule of thumb

   The reduction of the wing root bending moment through use of MLA/GLA can be associated with a weight saving in *kg* from prior experience and statistics. A dedicated sizing procedure is not necessary.

2. Sizing with the actively reduced loads without load loops

   The loads from the closed loop loads analysis are used for the sizing of the aircraft. This procedure is carried out once and the updated mass due to alleviated loads is obtained.

3. Sizing with the actively reduced loads with a load loops

   Since the sizing procedure changes the mass and the stiffness of the wing, the loads analysis has to repeated with the updated structural model. This procedure has to be repeated until a convergence is reached. These are the so called loads loop. Typically this process converges in about 3 to 4 iterations.

11 Wing Shape Control and Lift over Drag

In order to determine an overall lift distribution with minimal drag for a given fuel state, an optimization is carried out to obtain a respective flap setting. Since there is no dedicated aerodynamic design process, the flap setting determined for the cruise performance mass case and flight point is used as an offset. This way a the non optimal twist distribution due toe the missing aero design procedure is accounted for.

We select a flight point (Ma=0.8, h=10000m, mass 80% payload, 50% fuel, mid cg) for the optimal wing shape control.

Performance Flap setting

For this case we trim for horizontal flight and determine a flap setting minimizing drag (This in lieu of a proper aero design). PANUKL is a software package to compute the aerodynamic characteristics using low order panel methods [5]. The PANUKL framework consists of several programs, four of which are used in this investigation. The four programs, in logical order are listed below.

- Mesh3: Generates the investigated geometry mesh.
- Neigh: Calculates the connections of the generated panel mesh elements.
- Panukl: Performs the aerodynamic calculations.
- Press: Defines the important variables (lift force, pitching moment, etc.)

To achieve true trim flight conditions, the elastic deformation of the flexible structure needs to be taken into account. In this case, surface spline theory is used, which enables the transformation of aerodynamic forces and moments to the structural model and structural deformation to the aerodynamic

model. The result is an iterative process with the undeformed aircraft geometry and structural properties as the input and the deformed geometry as the output. The software is run for several control surface deflection cases to obtain the optimal control surface deflection that minimize the drag. This CS deflection we call the Performance Flap Setting. The result of this block is the optimal control surface (CS) deflection with the corresponding C_D and C_L values. The initial configuration, where all ailerons are kept at zero degrees is called the Baseline Flap Setting.

The range increase is determined using the Performance and the Baseline Flap Settings, where the corresponding C_D, C_L values are inserted in the Breguet Range equation.

12 Performance evaluation

For performance evaluation the Breguet equation is used. This equation computes the range of an aircraft accounting for the fuel weight depleted during the mission and shows how the range can be increased as a function of the aircraft parameters. There are three physical effects considered in the equation. The propulsion efficiency, which is not addressed in the current study. The structural weight of the aircraft, which can be reduced by load alleviation functions and relaxed stiffness requirements due to the active flutter suppression system. And finally, the aerodynamic efficiency which can be improved by employing an active wing shape control function.

Breguet equation is given by

$$R = \frac{C_L}{C_D} \cdot \frac{V}{b_f g} \cdot \ln\left(\frac{m_0}{m_0 - m_t}\right). \tag{3}$$

The mass cases are provided along the mission trajectory according to the consumption of fuel in the wing tanks. For each of the mass cases an optimal L/D is calculated with the procedure described above. The resulting ranges are then sum up and serve as metric for comparison of the performance of the designs. For the design without wing shape control, the flap setting for the performance point with 50 % fuel is used throughout the mission.

13 Flutter Assessment and Active Flutter Suppression

Some designs might be prone to flutter within the extended flight envelope. The linearized LTI state space models from the dynamic model generation are used to determine if a design flutters. If a design flutters an active flutter suppression control laws is designed to push the flutter speed beyond the critical extended flight envelope boundary if possible.

Three outcomes are possible:

- no flutter: There is no flutter within the flight envelope;
- controllable flutter: The is open loop flutter and the controller successfully suppressed it beyond the boundary of the flight envelope;
- uncontrollable flutter: the controller is unable to suppressed flutter within the boundary of the flight envelope.

The first step of the flutter control design tool is first to evaluate weather the open loop model contains unstable flutter dynamics. If this condition holds, a flutter control needs to be synthesized based on

the LTI model of the open loop model. The LTI model of the aircraft is is obtained via the ASE model integration block via Jacobian linearization. The linearization needs to be carried out in a way such that time delays, actuator and sensor states are not incorporated in the model. Since the LTI model is derived from the high-fidelity nonlinear ASE model, it has too many states for direct flutter suppression control design even without the actuator and sensor dynamics. Therefore, the first step is to reduce the order of the states. This is achieved by truncating and residualizing rigid body states that do not contribute to the flutter mechanism, after which a balanced realization is done. The balanced realization results in an LTI representation in which the states contributing to the input/output behavior of the model are sorted in descending order. The states contributing the leas to the input/output behavior are then residualized. The input of the flutter controller consists of the pitch rate (q), and angular rate measurement from the IMU sensors (q_L and q_R) placed along the wing. The actuating signals are the deflection commands for the pair of outermost ailerons. Once the inputs and outputs for the control design are defined, the corresponding actuator/sensor dynamics with the Pade approximation of the time delay is added to the model. The controller is designed for this reduced order model with structured H_∞ synthesis. The state-space model of the resulting flutter suppression controller is the output of the block.

The analysis of the closed-loop is based on disk margin calculations. Complex scalar uncertainties are injected into the channels involved in the feedback loops and the phase and gain combination at which the closed-loop becomes unstable is computed in each channel, simultaneously. The results of the flutter controller analysis block is the open loop flutter speed and the robust closed loop flutter speed.

14 Results

In this chapter the results of the described workflow are presented. In order to assess the benefits of the different active control technologies implemented several permutations of the active respectively non-active control laws will be compared.

14.1 Active load alleviation benefits

It has been shown in [6] that for the D150 aircraft active load alleviation in the preliminary aircraft design stage can yield a significant reduction of wing box mass. The active load alleviation methods presented in [6] resulted in 6.2% less wing root bending moment using MLA and 10.7% less bending moment at the root of the active aircraft using GLA. This can lead to a wing structural mass reduction of 130.5 kg (0.18% of MTOM, 0.32% of OEM). The MLA and GLA methods presented in this report lead to approximately 20% decrease in the wing root bending moments with respect to the the open-loop gust loads. Based on these active load alleviation methods, the possible wing mass reduction is assumed to be approximately double of the amount of [6], which is a reduction of 260 kg. Therefore, the following values are used for the redesigned wing parameters, as given in Table 2.

Table 2: Main parameters of the D150 baseline (reference) and redesign configuration

	Reference aircraft	**Redesigned aircraft**
Operational empty weight (OEM)	40638 kg	40508 kg
Maximum zero-fuel weight (MZFM)	60500 kg	60240 kg
Maximum take-off weight (MTOM)	72500 kg	72240 kg
Take-off fuel	10450 kg	10450 kg
Cruise Mach number	0.8	0.8

The performance of utilizing active load alleviation methods is evaluated based on the range increase of the redesigned aircraft. This evaluation is done using the Breguet equation.

Table 3: Main parameters and range results of the D150

	Reference aircraft	**Redesigned aircraft**
Take-off fuel	10450 kg	10450 kg
Take-off mass, m_0	71000 kg	70740 kg
Landing mass (10% fuel remaining)	61595 kg	61335 kg
Fuel consumed, m_t	9405 kg	9405 kg
Cruise Mach number	0.8	0.8

The Breguet equation indicates that with active load alleviation, the range of the D150 can be extended by 0.4%. If the range is to be kept as for the initial aircraft configuration, then the saved wing mass can be utilized for more passenger seats.

14.2 Wing shape control benefits

PANUKL results for the D150 aircraft

The goal is to use PANUKL to obtain the induced drag values for the reference aircraft (with zero aileron deflections) and the minimal induced drag corresponding to the optimal aileron configuration. It is assumed that the aircraft has 10 ailerons as shown in Figure 11.

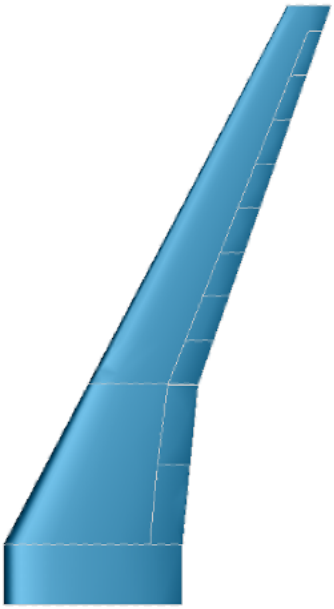

Figure 11: 10 aileron configuration of the D150 aircraft

PANUKL is configured in the following way:

- Mach: 0,8; Altitude: 10 km
- 2800 simulations: Investigated angles [-1...1,5] degrees
- Outputs: C_{Di} and C_L values for each aileron combination

PANUKL results:

- C_{Di} for the reference case: 2.705×10^{-3}
- C_{Di} for the optimal aileron setup: 2.543×10^{-3}

The optimal aileron deflections are given in Table 4.

Table 4: Optimal aileron deflections

Ailerons	A1	A2	A3	A4	A5	A6	A7	A8	A9	A10
degrees	0	1	1.5	1	1	2	1	2	0.5	0

Substituting the results of the optimized induced drag and reference induced drag models, the Breguet equation indicates 6.37% range increase compared to the reference aircraft model. Note that since induced drag values are substituted into the Breguet equation instead of the drag coefficient, the range increase using optimal aileron configuration can lead to a smaller increase in real implementation.

14.3 Flutter assessment

For the reference aspect ratio, there were no unstable flutter modes.

15 Bibliography

[1] Raymond L. Bisplinghoff, Holt Ashley, and Robert L. Halfman. *Aeroelasticity*. Dover Publications, Inc., 1955.

[2] Emilio M Botero, Andrew Wendorff, Timothy MacDonald, Anil Variyar, Julius M Vegh, Trent W Lukaczyk, Juan J Alonso, Tarik H Orra, and Carlos Ilario da Silva. SUAVE: An open-source environment for conceptual vehicle design and optimization. In *54th AIAA aerospace sciences meeting*, page 1275, 2016.

[3] European Aviation Safety Agency. Certification specifications for large aeroplanes (cs-25). 2007.

[4] Edward H. Frank and Jim Lyle. *Type-Certificate Data Sheet No. EASA.A.064 for Airbus A318-A319-A320-A321*. European Aviation Safety Agency, 2012.

[5] Tomasz Grabowski. Panukl, 2022.

[6] Vega Handojo. *Contribution to Load Alleviation in Aircraft Pre-design and Its Influence on Structural Mass and Fatigue*. PhD thesis, Deutsches Zentrum fuur Luft- und Raumfahrt Institut fuur Aeroelastik, Gottingen, 2020.

[7] Thiemo Kier and Gertjan Looye. Unifying manoeuvre and gust loads analysis models. In *International Forum on Aeroelasticity and Structural Dynamics*, 2009.

[8] Thomas Klimmek. *Statische aeroelastische Anforderungen beim multidisziplinären Strukturentwurf von Transportflugzeugflügeln*. PhD thesis, DLR - Institut für Aeroelastik, 2016.

[9] Thomas Klimmek, Matthias Schulze, Mohammad Abu-Zurayk, Caslav Ilic, and Andrei Merle. cpacs-MONA – An independent and in high fidelity based MDO tasks integrated process for the structural and aeroelastic design for aircraft configurations. In *International Forum on Aeroelasticity and Structural Dynamics 2019, IFASD 2019*, Juni 2019.

[10] Matthias Schulze, Jens Neumann, and Thomas Klimmek. Parametric modeling of a long-range aircraft under consideration of engine-wing integration. *Aerospace*, 8(1):1–20, 2021.

[11] Thomas Zill, Pier Davide Ciampa, and Björn Nagel. Multidisciplinary design optimization in a collaborative distributed aircraft design system. In *50th AIAA Aerospace Sciences Meeting including the New Horizons Forum and Aerospace Exposition*, page 553, 2012.